

Hot Paper

CaLi₂PN₃ – A Quaternary Chain-Type Nitridophosphate by Medium-Pressure SynthesisReinhard M. Pritzl,^[a] Nadine Fahle,^[a] Kristian Witthaut,^[a] Sebastian Wendl,^[a] and Wolfgang Schnick*^[a]

Nitridophosphates are in the focus of current research interest due to their structural versatility and properties, such as ion conductivity, ultra-incompressibility and luminescent properties when doped with suitable activator ions. Multinary representatives often require thorough investigation due to the competition with the thermodynamically more stable binary and ternary compounds. Another point of concern is the synthetic control of structural details, which is usually limited by conventional bottom-up syntheses. In this study, we report on the synthesis and characterization of the quaternary nitridophosphate CaLi₂PN₃. Various synthesis protocols were used for the preparation of CaLi₂PN₃, including the novel nitridophosphate double salt approach. The crystal structure was solved and

refined from single-crystal X-ray diffraction data and confirmed by Rietveld refinement, solid-state NMR spectroscopy, EDX measurements and low-cost crystallographic calculations. The experimental results were corroborated by DFT calculations, which revealed the electronic band structure. Formation energy calculations allowed conclusions to be drawn about the stability in comparison to the initial ternary nitridophosphates. The synthesis of CaLi₂PN₃ exemplifies the enormous potential of medium-pressure syntheses in the field of nitridophosphate research. Furthermore, the presented new synthesis route allows a certain degree of structural control, which is a promising addition to previous synthesis strategies in nitridophosphate chemistry.

Introduction

Nitridophosphates exhibit a multifaceted structural diversity with structural motifs similar to those of oxosilicates. In recent years, a large number of representatives has been prepared using various synthetic approaches. These range from (pressure) ampoules, hot isostatic press (HIP) to multianvil press (LVP) or diamond anvil cell synthesis.^[1–6] In this context a number of synthetic strategies and synthesis protocols has been developed. For instance, the nitride/azide routes, metathesis reactions, and the Li₃N self-flux have been established.^[7] Nonetheless, the influence of these bottom-up synthesis methods on the structural details is limited. The degree of condensation κ (i.e. ratio of tetrahedra centers (P) and ligands (N)) can be influenced by selecting the stoichiometry of the reactants, which is oriented on the desired molecular formula.^[8,9] However, the post-synthetic modification developed by Wendl et al. allows for a certain extent of synthetic control.^[10] In contrast to the classic bottom-up approaches, a top-down approach was developed. Ion exchange reactions were conducted by reacting pre-synthesized alkaline earth metal nitridophosphates with

other metal halides under elevated pressure. In addition to topotactic ion exchange, atomic rearrangements were also observed, which resulted in the formation of different P/N substructures or structure types in general. A comparison of all previously mentioned routes reveals that elevated pressure is beneficial for synthesis. The challenge of nitridophosphate synthesis is primarily due to the limited thermal stability of nitride precursors, such as P₃N₅, and the desired products.^[11] Thermal decomposition is usually prevented by increasing the synthesis pressure (*SP*). A more detailed examination of the literature reveals a trend indicating less harsh reaction conditions in terms of *SP* are required for lowly-condensed nitridophosphates ($\kappa < 1/2$) than for highly condensed representatives ($\kappa \geq 1/2$).^[9,12–14] For example MP₂N₄ (*M*=Ge, Be, Cd, Mn, Ca, Sr, Ba) and MP₈N₁₄ (*M*=Fe, Co, Ni, Mg, Ca, Sr, Ba) have only been prepared in the GPa regime, while Li₇PN₄, Li₁₂P₃N₉, Mg₂PN₃, Ca₂PN₃ and Sr₃P₃N₇ are attainable using pressure ampoules or ammonothermal reaction conditions.^[10,12,14–22] All of the latter representatives have isolated anionic structural motifs in common, namely infinite vertex-sharing chains of PN₄ tetrahedra. A comparison of this chain motifs reveals that the simplest case observed in nitridophosphates is unbranched *zweier*-single chains (based on Liebau's nomenclature for silicates).^[23] These have so far been observed in the absence of additional network-forming cations *NFC* (*NFC*=additional, tetrahedrally coordinated cations) in Ca₂PN₃ (ambient conditions, ampoules), Li₄PN₃ (high-pressure conditions, LVP), and have recently been reported in GePN₃ (ultra-high-pressure conditions, diamond anvil cell (DAC)).^[6,12,14] This observation was our starting point to search for novel quaternary chain-type nitridophosphates. A synthesis under medium-pressure conditions where both lithium and calcium are present as counter cations appears to offer

[a] R. M. Pritzl, N. Fahle, K. Witthaut, S. Wendl, W. Schnick
Department of Chemistry, University of Munich (LMU), Butenandtstraße 5–13, 81377 Munich, Germany
E-mail: wolfgang.schnick@uni-muenchen.de

Supporting information for this article is available on the WWW under <https://doi.org/10.1002/chem.202402521>

© 2024 The Author(s). Chemistry - A European Journal published by Wiley-VCH GmbH. This is an open access article under the terms of the Creative Commons Attribution Non-Commercial NoDerivs License, which permits use and distribution in any medium, provided the original work is properly cited, the use is non-commercial and no modifications or adaptations are made.

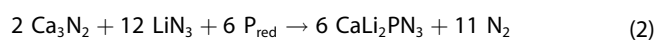
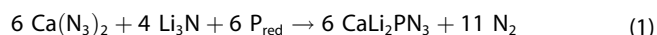
a promising starting point for further research. In this contribution, we report on synthesis and structural investigation of CaLi_2PN_3 , the first quaternary alkaline/alkaline earth metal nitridophosphate. Two distinct synthesis approaches are presented: A well-established bottom-up approach, which involves the use of azide/nitride precursors and a novel, exploratory top-down double salt approach using nitridophosphate-based chain-type precursors, with the objective of retaining the anionic structural motifs. We have succeeded in growing single crystals suitable for structure determination using single-crystal X-ray diffraction data and provide a comprehensive structural analysis by combining PXRD, SEM-EDX, MAS NMR and low-cost crystallographic calculations (LCC). Formation energy calculations and the calculation of the band structures complement the characterization.

Results and Discussion

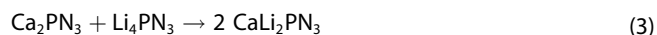
Synthesis

CaLi_2PN_3 was obtained by solid-state medium-pressure reactions at 900 °C and 200 MPa under N_2 atmosphere (Experimental Section). Two different synthesis strategies were identified as optimal after empirical optimization (A and B):

A) Bottom-up synthesis using the nitride/azide route:



B) Top-down double salt synthesis using pre-synthesized chain-type nitridophosphates:



According to Equations (1–3), different amounts of CaLi_2PN_3 were obtained together with varying amounts of Ca_2PN_3 , $\text{Li}_{10}\text{P}_4\text{N}_{10}$ and CaO . The results of the corresponding Rietveld refinements can be found in Figures S1&S2 and Table S1. The highest phase portions were obtained by Equation (1), however, unassignable reflections observed in the powder diffraction of the bottom-up syntheses indicate the presence of unknown minor side phase(s). The elucidation of this is subject of future research. According to Equations (1) and (2), the use of metal azides is necessary for bottom-up synthesis, as no CaLi_2PN_3 was formed using only nitrides as starting materials ($\text{P}_{\text{red}}/\text{P}_3\text{N}_5$, Li_3N , Ca_3N_2).

The best results for the synthesis were obtained at temperatures of 880–900 °C, which seems to be a compromise for the synthesis temperatures of many lithium nitridophosphates (α -/ β - $\text{Li}_{10}\text{P}_4\text{N}_{10}$ (T : 630–720 °C), LiPN_2 (T : 800 °C), $\text{Li}_{12}\text{P}_3\text{N}_9$ (T : 790 °C) or the high-pressure polymorph Li_4PN_3 (T : 820 °C) and Ca_2PN_3 (T : 1200 °C).^[2,12,14,24–26]

The title compound was isolated as colorless crystals (up to 30 μm in length, Figure 1) that are sensitive to air or moisture. In order to select suitable crystals for single-crystal structure

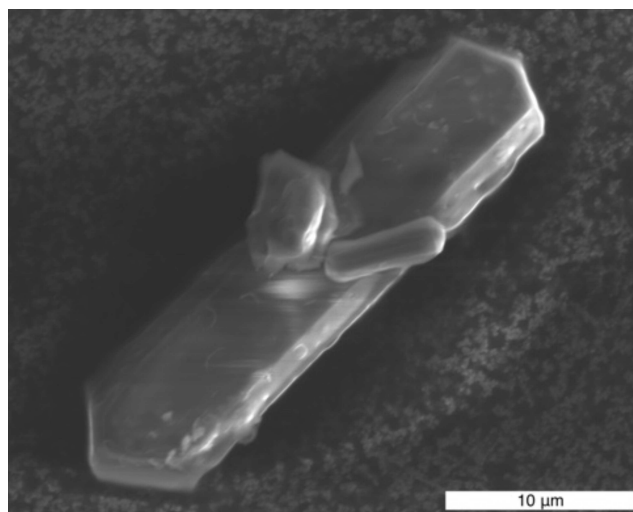


Figure 1. SEM image of an isolated single-crystal of CaLi_2PN_3 .

analysis (SCXRD) and to distinguish them from the minor side phases (detected by PXRD), their photoluminescence properties were exploited by doping with Eu^{2+} . Crystals of the side phase $\text{Ca}_2\text{PN}_3:\text{Eu}^{2+}$ show a deep red emission with $\lambda_{\text{em, max}} = 650 \text{ nm}$ upon irradiation with UV to blue light.^[2] For this purpose, small amounts of EuCl_2 (~1 mol% with respect to Ca^{2+} according Equation (2)) were added during synthesis. At room temperature, CaLi_2PN_3 does not exhibit any discernable luminescent properties when irradiated with UV to blue light.

Structure Elucidation

The crystal structure of CaLi_2PN_3 was solved and refined from single-crystal X-ray diffraction data. CaLi_2PN_3 crystallizes in monoclinic space group $C2/c$ (no. 15) with eight formula units per unit cell and lattice parameters $a = 11.3397(4)$, $b = 11.5881(4)$, $c = 4.9408(2) \text{ \AA}$, $\beta = 113.966(1)^\circ$ (Table 1, Experimental Section).^[27]

All atomic positions were determined during the structure solution process and the displacement parameters are refined anisotropically (Wyckoff positions, atomic coordinates, anisotropic displacement parameters, interatomic distances and angles are given in Tables S2–S5). Solid-state ^{31}P MAS spectroscopy experiments support the proposed structure model with phosphorus on one independent crystallographic site (Wyckoff 8f). The observed chemical shift $\delta = 15.1 \text{ ppm}$ ($fwhm = 4.2 \text{ ppm}$, Figures S3–S5) is in a typical range for lithium (oxo)nitridophosphates and also partially observed in alkaline earth metal nitridophosphates.^[24,28–30] The consistency observed in both distinctive compound classes can serve as a benchmark for future mixed alkaline/alkaline earth nitridophosphates. ^6Li & ^7Li MAS spectra confirm the presence of lithium in the prepared samples (Figures S6&S7). However, due to the small chemical shift differences of the $^6/7\text{Li}$ MAS NMR signals, no clear differentiation from the signals of the Li containing side phases is possible. In order to prove the absence of imide functionality

Table 1. Crystal data for CaLi_2PN_3 ; estimated standard deviations are given in parentheses.	
Formula	CaLi_2PN_3
Crystal system	monoclinic
Molecular weight/ g mol^{-1}	253.92
Space group	$C2/c$ (no. 15)
Lattice parameters/ \AA , $^\circ$	$a = 11.3397(4)$ $b = 11.5881(4)$ $c = 4.9408(2)$ $\beta = 113.966(1)$
Cell volume/ \AA^3	593.28(4)
Formula units per cell	8
Calculated density/ g cm^{-3}	2.843
μ/mm^{-1}	2.378
$T_{\text{min}}/T_{\text{max}}$	0.958/1.000
Radiation	Mo-K α ($\lambda = 0.71073 \text{ \AA}$)
Temperature/K	293(2)
$F(000)$	496
θ range/ $^\circ$	$3.516 < \theta < 28.694$
Total no. of reflections	5109
Independent reflections ($> 2\sigma$)	764 (734)
Refined parameters	65
$R_{\text{int}}; R_\sigma$	0.0252; 0.0164
$R1$ (all data); $R1$ ($F^2 > 2\sigma(F^2)$)	0.0175; 0.0165
$wR2$ (all data); $wR2$ ($F^2 > 2\sigma(F^2)$)	0.0421; 0.0417
Goodness of fit	1.121
$\Delta\rho_{\text{max}}; \Delta\rho_{\text{min}}/\text{e \AA}^{-3}$	0.362; -0.314

(N–H) in the title compound $^{31}\text{P}\{^1\text{H}\}$ NMR experiments were performed (Figures S8&S9). The observed signals do not correspond to any of the positions of the signals in the direct ^{31}P spectra, which suggests there is no hydrogen present in CaLi_2PN_3 . Nevertheless, the observed signals indicate that the minor unknown side phases contain imide/amide groups. To confirm the elemental composition, SEM-EDX investigations were carried out on selected crystallites. Only the atomic cation ratios were considered, as the tendency for hydrolysis falsifies both the anion and total atomic values. The measured values are consistent with the theoretical values and are within the typical error range of this method, thereby corroborating the elemental composition (Table S6). The electrostatic plausibility of the crystal structure was analyzed by various low-cost crystallographic calculations, including bond-valence sums (BVS) and charge distribution (CHARDI) calculations (Tables S7&S8).^[31–33] These confirm the consistency of the structure model.

Structure Description

As expected for $\kappa = 1/3$ CaLi_2PN_3 consists of infinite *zweier*-single-chains of vertex-sharing PN_4 -tetrahedra, running along c ,

with $[\text{PN}_2\text{N}_{2/2}]^{4-}$ according to Niggli.^[34] Simplified, the structure can be described as a cationic filling variant of the recently reported nitridophosphate $\text{Ge}^{\text{IV}}\text{PN}_3$, which crystallizes in the CoGeO_3 structure type, synthesized under high-pressure conditions (approx. 44 GPa).^[6,35] A structural overview is shown in Figure 2.

Given that CaLi_2PN_3 is formally composed of the chain-type nitridophosphates Ca_2PN_3 (synthesized at ambient pressure conditions) and Li_4PN_3 (synthesized at high-pressure conditions), it is advisable to undertake a comparison with the other two compounds (Figure 3). However, it should be noted that these three compounds do not share the same reference coordinate system with regard to the direction of the anionic chains. In order to facilitate a more accurate comparison, a new coordinate system is introduced, whereby the x -axis points in the direction of the individual *zweier*-chains, the y axis in the direction of the alignment of the unbridged terminal $\text{N}^{(1)}$ and the z -axis in the direction of the layer sequence. All three compounds comprise a single P site, which has the consequence that the resulting chains within a distinct compound can be converted into each other solely by means of symmetry operations (for the sake of clarity, only inversion centers are illustrated in Figure 3, the chain arrangement section). This approach facilitates a straightforward comparison of the chains in terms of their arrangement, alignment (inclination) and elongation. To gain a more comprehensive understanding, it is essential to initially examine the elongation of the PN_4 -tetrahedra chains. This can be quantified by the stretching factor $f_s = l_{\text{chain}}/(l_T \times P)$, which was originally introduced by Liebau for the classification of chain silicates.^[23] The definition of l_{chain} and l_T is provided in Figure 2b. The periodicity $P=2$, as expected for *zweier*-single-chains, leads to maximally stretched

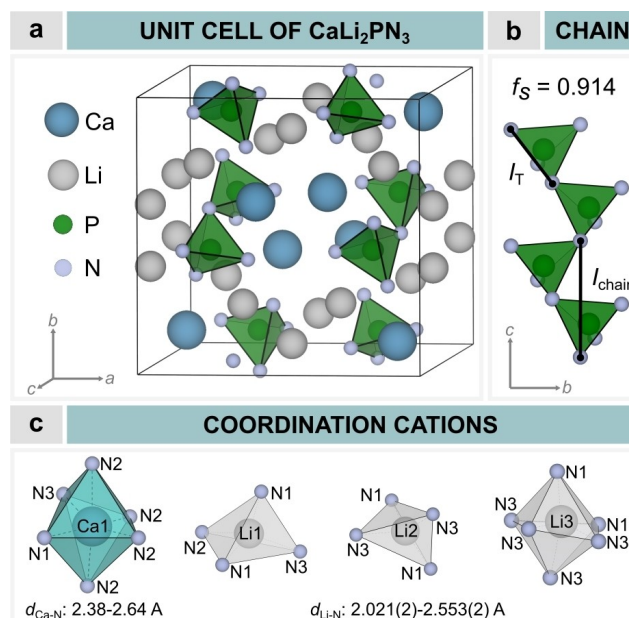


Figure 2. Structure model of CaLi_2PN_3 ; a) unit cell with PN_4 tetrahedra-motif in green, Ca atoms in blue, Li atoms in gray, N atoms in light-blue; b) PN_4 -tetrahedra chain with stretch factor (and respective parameters); c) coordination spheres of Ca (cyan) and Li (gray) atoms in CaLi_2PN_3 .

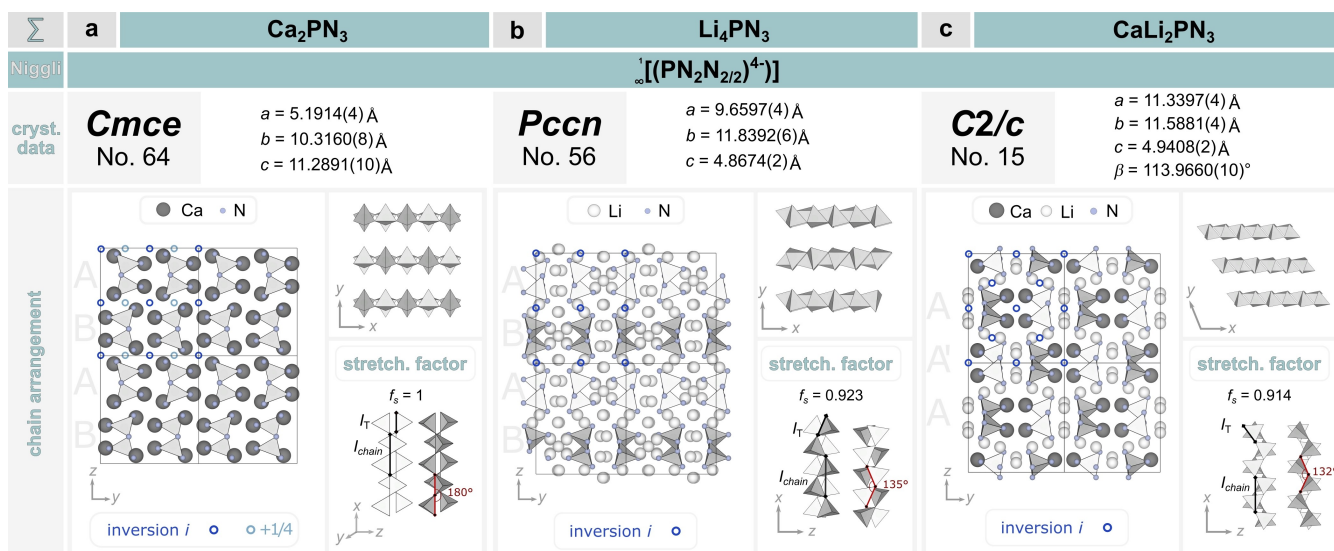


Figure 3. Structural comparison of the chain-type nitridophosphates Ca_2PN_3 (a), Li_4PN_3 (b) and CaLi_2PN_3 (c) in terms of their chain arrangement and stretching factor. PN_4 -tetrahedra chains in gray; saw-tooth arrangement into the plane (bright) and out of the plane (dark).

(=relaxed) chains with $f_s = 1$ for Ca_2PN_3 , to less stretched chains with $f_s = 0.923$ for Li_4PN_3 and to the most compressed chains within this series of compounds with $f_s = 0.914$ for CaLi_2PN_3 (Figure 2b).^[12,14] Less stretched PN_4 -tetrahedra *zweier*-chains have been reported for Mg_2PN_3 and Zn_2PN_3 .^[12,36] Examination of the P–N distances ($d_{\text{P-N}} = 1.61\text{--}1.72\text{Å}$) shows that these are within the typical range for nitridophosphates.^[37–39] As expected, the distances to the terminal $\text{N}^{[1]}$ ($1.6084(12)\text{Å}$ and $1.6268(13)\text{Å}$) are significantly shorter than to the bridging $\text{N}^{[2]}$ ($1.7147(14)\text{Å}$ and $1.7269(12)\text{Å}$). This compression is reflected in the P–N–P angles of the respective chains, with CaLi_2PN_3 having the most acute angle with P–N–P = $123.44(8)^\circ$. The compression also allows the chains to be distinguished in terms of their inclination along the x -axis. To better illustrate this, the color code gray and white was chosen in Figure 3 to achieve maximum contrast. The chains can be classified into two groups: those whose sawtooth arrangement points into the plane (Figure 3, dark chains) and those whose arrangement leads out of the plane (Figure 3, bright chains). It is not possible to classify the chains of Ca_2PN_3 in this context due to the maximum elongation. Furthermore, a classification can be made with regard to the orientation of the terminal $\text{N}^{[1]}$ atoms. This results in different arrangement patterns, which can be classified into layer sequences along z : Ca_2PN_3 : A-B-A; Li_4PN_3 : A-B-A and CaLi_2PN_3 : A-A'-A. In the case of CaLi_2PN_3 the following layer can be formed by translation of $1/2$ in y direction. When all the above classification criteria are combined, a kind of checkerboard pattern emerges in the case of CaLi_2PN_3 , which is absent in either of the other two compounds. This arrangement and alignment of the chains result in CaLi_2PN_3 exhibiting areas dominated by unbridged $\text{N}^{[1]}$ and areas dominated by bridged $\text{N}^{[2]}$ comparable to Li_4PN_3 . The divalent Ca^{2+} ions are localized in the former and are coordinated in a distorted octahedral fashion by six nitrogen atoms ($\text{CN} = 6$, $d_{\text{Ca-N}} = 2.3468(12)\text{--}2.6367(11)\text{Å}$; Figure 2c).

The interatomic distances are slightly shorter compared to the distances described in the literature for Ca_2PN_3 ($d_{\text{Ca-N}} = 2.4331(13)\text{--}3.0074(11)\text{Å}$), but on average these correspond to the sum of the respective Shannon radii.^[12,40]

However, to enable a more accurate comparison of the coordination polyhedral, minimum bounding ellipsoid analysis (MBE) was performed for both Ca_2PN_3 and CaLi_2PN_3 .^[41] The basis of MBE, the ellipsoidal approximation, enables the comparison of the distortion of different polyhedra, especially irregular ones based on the bonding distances. Consequently, the Ca^{2+} coordination polyhedra in Ca_2PN_3 can be described as distorted pentagonal bipyramids ($\text{CN} = 7$) and as distorted square pyramids ($\text{CN} = 5$). Therefore, the CaN_6 octahedra in CaLi_2PN_3 represent an average in CN of the two polyhedra of Ca_2PN_3 and are significantly less distorted (Figures S10&S11, Tables S9&S10). In combination with the reduced Ca^{2+} polyhedron volume, this could be a plausible explanation for the absence of luminescence behavior, as previously outlined in the synthesis section. The given possible dopant position is very small and therefore unfavorable for an occupation by Eu^{2+} ions.^[42] The Ca^{2+} octahedra are connected to each other by common vertices and edges and share also edges and vertices with PN_4 -tetrahedra. Three PN_4 tetrahedra-chains are connected to each other by one Ca^{2+} octahedron. A partial topological representation (Figure S12) also allows the arrangement of Ca^{2+} between the PN_4 tetrahedra-chains to be described as sawtooth-like (the shortest Ca–Ca distances ($d_{\text{Ca-Ca}} = 3.2291(5)\text{Å}$) are connected as a blue line). Li^+ ions are coordinated by nitrogen with $\text{CN} = 4$ (Li1 and Li2) and 6 (Li3), as determined by MBE.^[41] The resulting polyhedra share common corners and/or edges, resulting also in a sawtooth-like arrangement (Figure S13).

Density Functional Theory Calculations (DFT)

Given the unavailability of a phase-pure synthesis of the title compound and the consequent limitation of the experimental analysis, we have decided to conduct periodic DFT calculations.^[43–45] The calculated band structures (Figure 4) and densities of states (DOS, Figure S14) indicate that CaLi_2PN_3 is an electronically wide band gap semiconductor. The theoretical indirect band gap is estimated to be 3.35 eV, which is comparable to that of ZnO (direct band gap: 3.37 eV) and GaN (direct band gap: 3.40 eV).^[46,47] The indirect transition between valence band (between V and Γ point) and the conduction band minimum (at V point) is shown (green arrow). Near the Fermi level (shifted to 0 eV), the contributions primarily originate from 2p states of N. On the other hand, the total DOS in the conduction band is almost exclusively dominated by the contribution of Ca (3d), whereas the contributions of P and N are negligible.

In addition to the electronic properties, the stability of CaLi_2PN_3 was investigated by calculating the formation energy E_{form} from the total energies E_{tot} of the constituent compounds Li_4PN_3 and Ca_2PN_3 according to Equation (4):

$$\Delta_f E = E_{\text{tot}}(\text{CaLi}_2\text{PN}_3) - E_{\text{tot}}(\text{Li}_4\text{PN}_3) - E_{\text{tot}}(\text{Ca}_2\text{PN}_3) \quad (4)$$

These calculations show that the formation of CaLi_2PN_3 results in an energy gain relative to the two starting nitridophosphates. This is evident by the formation energy per formula unit $\Delta_f E = 13.75$ eV (Table S11). A potential explanation for the notable enhancement in stability relative to the compounds Li_4PN_3 and Ca_2PN_3 is the less distorted Ca^{2+} coordination environment accompanied by the previously described significantly shorter bond distances, as well as the less distorted Li positions, analyzed by MBE.

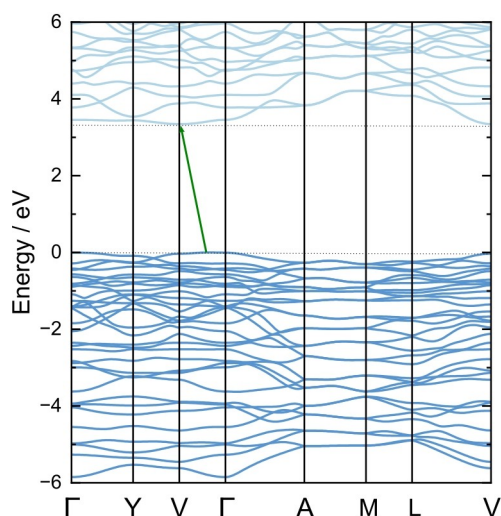


Figure 4. Calculated band structure of CaLi_2PN_3 . Green arrow indicates the indirect transition (indirect band gap).

Conclusions

In this contribution, we report on the successful preparation of the first quaternary lithium alkaline-earth nitridophosphate, CaLi_2PN_3 , via MP/HT synthesis. The azide route established for nitridophosphate synthesis and a for nitridophosphate synthesis novel double salt approach were employed to prepare the title compound with different phase content. Single-crystals suitable for structure elucidation allowed the crystal structure to be determined from single-crystal X-ray diffraction data. The elemental ratio determined by EDX analysis on selected crystallites is consistent with the proposed structure model. Solid-state MAS NMR analysis and low-cost crystallographic calculations support the obtained results. The crystal structure can be described as a novel cation-filling variant of GePN_3 , which crystallizes in the CoGeO_3 structure type. In terms of structural chemistry, it can be regarded as a combination of the low-pressure compound Ca_2PN_3 and the high-pressure compound Li_4PN_3 . This is experimentally supported by the aforementioned double salt synthesis. The experimental results were corroborated by quantum chemical calculations, which also revealed the electronic structure (indirect band gap ~ 3.35 eV). Furthermore, calculations were conducted to determine the formation energies of the title compound and the two separate nitridophosphates. These calculations support the plausibility of the proposed structural model and contribute to the understanding of the formation during synthesis. In summary, we were able to synthesize and structurally elucidate a novel quaternary nitridophosphate by comparing structural motifs and combine them in a novel compound by medium-pressure synthesis. The presented synthesis strategy offers considerable potential for further exploration of low-condensed nitridophosphates through the controlled combination and stabilization of pre-synthesized structural motifs (e.g. non-condensed $[\text{PN}_3]^{4-}$, $[\text{PN}_4]^{7-}$ or $[\text{P}_3\text{N}_9]^{12-}$ anions) under medium pressure conditions.

Experimental Section

Preparation of Starting Materials

Synthesis of $\text{Ca}(\text{N}_3)_2$

$\text{Ca}(\text{N}_3)_2$ was synthesized by an ion exchange reaction of CaCO_3 (Sigma Aldrich, 99.995 %) with aqueous HN_3 according to Suhrmann et al.^[48] The aqueous HN_3 was formed by passing an aqueous solution of NaN_3 (Acros Organics, 99%, extra pure) through a cation exchanger (Amberlyst 15). The solution was carefully dropped into an aqueous suspension of CaCO_3 until the eluate exhibited $\text{pH} = 7$. Residues of the carbonate was filtered and the solvent removed *in vacuo*. $\text{Ca}(\text{N}_3)_2$ was obtained as colorless crystals, which were investigated for phase-purity by powder X-ray diffraction. **Caution:** HN_3 required special care when handling. Special care must also be taken with diluted solutions, as these are extremely explosive and produce vapors that are toxic if inhaled.

Synthesis of P_3N_5

Semi-crystalline P_3N_5 was prepared through ammonolysis reaction of P_4S_{10} (Sigma Aldrich, 99.99%) with pre-dried NH_3 (Air Liquide, 5.0) according to Stock and Grüneberg.^[49] For this purpose, a quartz boat was placed in a tube furnace and dried at 1000 °C under reduced pressure of 10^{-3} mbar. After a cooling down step, the quartz boat was loaded with approx. 7 g P_4S_{10} and the apparatus was saturated with NH_3 for 1 h and subsequently heated up to 850 °C with 10 K/min. The obtained P_3N_5 was analysed by PXRD and CHNS analysis.

Synthesis of $LiPN_2$

$LiPN_2$ was prepared according to a new synthesis protocol under medium-pressure/high-temperature conditions in a hot isostatic press (HIP, AIP6-30H, American Isostatic Presses, Inc., Columbus Ohio, USA). For this purpose, Li_3N (Rockwood Lithium, 94%) and P_{red} (Chempur, $\geq 99.999\%$) in a molar ratio 2:6 were ground together in Ar-filled glovebox (MBraun, < 1 ppm H_2O , < 1 ppm O_2). The reactants were filled in a tungsten crucible, closed by a lid and placed in the security crucible made of corundum. This assembly was closed with another lid and transferred into the pressure module of the HIP. The pressure was constantly increased up to 82 MPa. Subsequently the reaction temperature was increased up to 1200 °C, ending with the reaction pressure of 200 MPa. After maintaining these conditions for 10 h, the sample was allowed to cool down to 20 °C and the pressure was released. The product was obtained as colourless sinter cake. After washing with water and ethanol the product was analysed by PXRD.

Synthesis of Li_4PN_3

Li_4PN_3 was prepared using high-pressure/high-temperature conditions using a modified Walker-type multianvil press (Voggenreiter, Mainleus, Germany). For this purpose a new synthesis protocol using Li_3N (Rockwood Lithium, 94%), $LiPN_2$ and P_3N_5 in a molar ratio of 5.25:1:1 was developed. The reaction was carried out at a reaction pressure of 8 GPa and a reaction temperature of 1000 °C for 60 min. More details on multianvil synthesis can be found in the literature.^[50] The obtained Li_4PN_3 was handled under inert-gas conditions and analysed by PXRD.

Synthesis of Ca_2PN_3

Ca_2PN_3 was prepared using medium-pressure/high-temperature conditions in a hot isostatic press (HIP, AIP6-30H, American Isostatic Presses, Inc., Columbus Ohio, USA). For this purpose, Ca_3N_2 (ABCR, 99%) and P_{red} (Chempur, $\geq 99.999\%$) in a molar ratio of 2:3 were reacted under a nitrogen atmosphere at 1200 °C and 150 MPa according to Wendl et al.^[2] Ca_2PN_3 was obtained as colorless/light beige sinter cake, handled under inert-gas conditions and analysed by PXRD.

Synthesis of $CaLi_2PN_3$

The title product was prepared under medium-pressure/high-temperature conditions in a hot isostatic press (HIP, AIP6-30H, American Isostatic Presses, Inc., Columbus Ohio, USA). For this purpose, the starting materials (in a molar ratio according to Equations 1–3) were ground together in an Ar-filled glovebox (MBraun, < 1 ppm H_2O , < 1 ppm O_2). The reactants were filled in a tungsten crucible, closed by a lid and placed in the security crucible made of corundum. This assembly was closed with another lid and transferred into the pressure module of the HIP. The pressure was

constantly increased up to 70 MPa. Subsequently the reaction temperature was increased up to 900 °C, ending with the reaction pressure of 200 MPa. After maintaining these conditions for 10 h, the sample was allowed to cool down to 20 °C and the pressure was released. The product was obtained as colourless crystals, which are sensitive against moisture and air.

Scanning Electron Microscopy (SEM) with Energy-Dispersive X-ray Spectroscopy (EDX)

The morphology and chemical composition of the title compound were investigated using a Helios Nanolab G3 UC (FEI, Hillsboro) dual-beam scanning electron microscope with an X-Max 80 SDD EDX detector (Oxford Instruments, Abingdon). For this purpose, the analysis samples were fixed on pre-dried carbon adhesive pads and carbon coated.

Solid-State Magic Angle Spinning (MAS) NMR Spectroscopy

^{31}P , 1H , $^{31}P\{^1H\}$, 6Li and 7Li NMR spectra were collected with a DSX AVANCE spectrometer (Bruker) with a magnetic field of 11.7 T. The samples were filled and compacted into a 2.5 mm rotor, which was mounted on a commercial MAS probe (Bruker). The sample was rotated at a rotation frequency of 20 kHz. The obtained data were analysed using ORIGIN Pro 2022b.

Single-Crystal X-ray Analysis (SCXRD)

SCXRD data were collected using combined ϕ - and ω -scans on a single-crystal of $CaLi_2PN_3$ on a D8 Venture TXS diffractometer (Bruker) with $Mo-K_{\alpha}$ radiation ($\lambda = 0.71073$ Å). The data were indexed, integrated, and absorption-corrected using the multi-scan method. The space group was determined using the APEX3 software package.^[51–53] The structure was solved using direct methods (SHELXT) and refined by full-matrix least square methods (SHELXL).^[54,55] The results were visualized using VESTA software.^[56]

Powder X-ray Diffraction (PXRD) and Rietveld Refinement

PXRD measurements were performed on pre-grounded samples of the bulk materials. These were pre-filled, compacted and sealed in glass capillaries (0.3 mm, Hilgenberg GmbH) under Ar atmosphere (Ar-filled glovebox; Unilab, MBraun, Garching, $O_2 < 1$ ppm, $H_2O < 1$ ppm). Measurements were performed on a Stoe STADI P diffractometer with $Cu-K_{\alpha 1}$ ($\lambda = 1.5406$ Å) radiation with Ge(111) monochromator and Mythen 1 K detector in modified Debye-Scherrer geometry. Subsequently, each data set was used for Rietveld refinement using the software TOPAS.^[57]

Quantum-Chemical Calculations (DFT)

Periodic density-functional theory (DFT) calculations were performed using the Vienna *ab initio* simulation package (VASP).^[43–45] In VASP the core and valence electrons are separated using projector-augmented waves (PAW).^[58,59] The exchange and correlation energy is calculated using the generalized gradient approximation (GGA), as described by Perdew, Burke and Ernzerhof (PBE).^[60] For the structure optimization (RMM-DIIS), the Brillouin zone was sampled on Γ -centered k -point grids ($4 \times 4 \times 7$ for $CaLi_2PN_3$, $7 \times 7 \times 3$ for Ca_2PN_3 and $3 \times 3 \times 6$ for Li_4PN_3) and the interpolation of the k space was done via tetrahedron method with Blöchl corrections.^[61] Full ionic degrees of freedom, i.e. atomic positions, cell shape and cell volume were used. Both Hellmann-Feynman forces and stress tensors were calculated. The energy convergence

criterion was set to 10^{-6} eV and the residual atomic forces were relaxed until the convergence criterion of 10^{-5} eV/Å was reached. Successive static calculations were performed with a convergence criterion of 10^{-8} eV and a plane wave energy cutoff of 500 eV. The band structure was calculated for the Bloch vector k along the lines Γ (0,0,0) to Y (−0.5,0,5,0) to V (0,0,5,0) to Γ (0,0,0) to A (0,0,0,5) to M (−0.5,0,5,0,5) to L (0,0,5,0,5) and back to V (0,0,5,0). The energy zero is taken at the Fermi level.

Acknowledgements

The authors thank Dr. Lisa Gamperl and Amalina T. Buda for carrying out SEM-EDX measurements and Christian Minke for NMR measurements (all at Department of Chemistry at LMU Munich). Open Access funding enabled and organized by Projekt DEAL.

Conflict of Interests

The authors declare no conflict of interest.

Data Availability Statement

The data that support the findings of this study are available in the supplementary material of this article.

Keywords: quaternary nitridophosphate · medium-pressure synthesis · solid-state structures · DFT · double salt synthesis

- [1] S. J. Sedlmaier, E. Mugnaioli, O. Oeckler, U. Kolb, W. Schnick, *Chem. Eur. J.* **2011**, *17*, 11258.
- [2] S. Wendl, S. Mardazad, P. Strobel, P. J. Schmidt, W. Schnick, *Angew. Chem. Int. Ed.* **2020**, *59*, 18240.
- [3] M.-H. Fang, H.-P. Hsueh, T. Vasudevan, W.-T. Huang, Z. Bao, N. Majewska, S. Mahlik, H.-S. Sheuc, R.-S. Liu, *J. Mater. Chem. C* **2021**, *9*, 8158.
- [4] R. M. Pritzl, M. M. Pointner, K. Witthaut, P. Strobel, P. J. Schmidt, W. Schnick, *Angew. Chem. Int. Ed.* **2024**, *63*, e202403648.
- [5] S. J. Ambach, M. Pointner, S. Falkai, C. Paulmann, O. Oeckler, W. Schnick, *Angew. Chem. Int. Ed.* **2023**, *62*, e202303580.
- [6] S. J. Ambach, G. Krach, E. Bykova, K. Witthaut, N. Giordano, M. Bykov, W. Schnick, *Inorg. Chem.* **2024**, *63*, 8502.
- [7] S. D. Kloß, W. Schnick, *Angew. Chem. Int. Ed.* **2019**, *58*, 7933.
- [8] G. Krach, J. Steinadler, K. Witthaut, W. Schnick, *Angew. Chem. Int. Ed.* **2024**, e202404953.
- [9] R. M. Pritzl, K. Witthaut, M. Dialer, A. T. Buda, V. Milman, L. Bayarjargal, B. Winkler, W. Schnick, *Angew. Chem. Int. Ed.* **2024**, e202405849.
- [10] S. Wendl, L. Seidl, P. Schüler, W. Schnick, *Angew. Chem. Int. Ed.* **2020**, *59*, 23579.
- [11] S. Horstmann, E. Irran, W. Schnick, *Z. Anorg. Allg. Chem.* **1998**, *624*, 620.
- [12] V. Schultz-Coulon, W. Schnick, *Z. Anorg. Allg. Chem.* **1997**, *623*, 69.
- [13] M. Mallmann, C. Maak, R. Niklaus, W. Schnick, *Chem. Eur. J.* **2018**, *24*, 13963.
- [14] E.-M. Bertschler, R. Niklaus, W. Schnick, *Chem. Eur. J.* **2017**, *23*, 9592.
- [15] M. Mallmann, S. Wendl, P. Strobel, P. J. Schmidt, W. Schnick, *Chem. Eur. J.* **2020**, *26*, 6257.
- [16] S. J. Ambach, C. Somers, T. de Boer, L. Eisenburger, A. Moewes, W. Schnick, *Angew. Chem. Int. Ed.* **2023**, *62*, e202215393.
- [17] F. J. Pucher, S. R. Römer, F. W. Karau, W. Schnick, *Chem. Eur. J.* **2010**, *16*, 7208.
- [18] F. J. Pucher, F. W. Karau, J. Schmedt auf der Günne, W. Schnick, *Eur. J. Inorg. Chem.* **2016**, *10*, 1497.
- [19] F. J. Pucher, A. Marchuk, P. J. Schmidt, D. Wiechert, W. Schnick, *Chem. Eur. J.* **2015**, *21*, 6443.
- [20] S. D. Kloß, O. Janka, T. Block, R. Pöttgen, R. Glaum, W. Schnick, *Angew. Chem. Int. Ed.* **2019**, *58*, 4685.
- [21] S. Wendl, L. Eisenburger, P. Strobel, D. Günther, J. P. Wright, P. J. Schmidt, O. Oeckler, W. Schnick, *Chem. Eur. J.* **2020**, *26*, 7292.
- [22] W. Schnick, J. Luecke, *J. Solid State Chem.* **1990**, *87*, 101.
- [23] The term *zweier* has been established by Liebau deriving from the German word of the numeral two (zwei (2)) by adding the suffix "er", describing the repeating structural units of tetrahedra. F. Liebau, *Structural Chemistry of Silicates: Structure, Bonding, and Classification*, Springer, Heidelberg **1985**, p. 58.
- [24] E.-M. Bertschler, C. Dietrich, T. Leichtweiß, J. Janek, W. Schnick, *Chem. Eur. J.* **2018**, *24*, 196.
- [25] W. Schnick, U. Berger, *Angew. Chem. Int. Ed.* **1991**, *30*, 830.
- [26] W. Schnick, J. Lücke, *Z. Anorg. Allg. Chem.* **1990**, *588*, 19.
- [27] Deposition Number 2365190 (for CaLi_2PN_3) contain the supplementary crystallographic data for this paper. These data are provided free of charge by the joint Cambridge Crystallographic Data Centre and Fachinformationszentrum Karlsruhe Access Structures service.
- [28] S. Schneider, S. Kreiner, L. G. Balzat, B. V. Lotsch, W. Schnick, *Chem. Eur. J.* **2023**, *29*, e202301986.
- [29] E.-M. Bertschler, R. Niklaus, W. Schnick, *Chem. Eur. J.* **2018**, *24*, 736.
- [30] R. M. Pritzl, N. Prinz, P. Strobel, P. J. Schmidt, D. Johrendt, W. Schnick, *Chem. Eur. J.* **2023**, *29*, e202301218.
- [31] I. D. Brown, *Chem. Rev.* **2009**, *109*, 6858.
- [32] A. Altomare, C. Cuocci, C. Giacovazzo, A. Moliterni, R. Rizzi, N. Corriero, A. Falcicchio, *J. Appl. Crystallogr.* **2013**, *46*, 1231.
- [33] M. Nespolo, B. Guillot, *J. Appl. Crystallogr.* **2016**, *49*, 317.
- [34] J. Lima-de-Faria, E. Hellner, F. Liebau, E. Makovicky, E. Parthe, *Acta Crystallogr.* **1990**, *A46*, 1.
- [35] D. R. Peacor, *Z. Kristallogr. Cryst. Mater.* **1968**, *126*, 299.
- [36] S. J. Sedlmaier, M. Eberspächer, W. Schnick, *Z. Anorg. Allg. Chem.* **2011**, *637*, 362.
- [37] S. Vogel, A. T. Buda, W. Schnick, *Angew. Chem. Int. Ed.* **2018**, *57*, 13202.
- [38] S. D. Kloß, W. Schnick, *Inorg. Chem.* **2018**, *57*, 4189.
- [39] E.-M. Bertschler, C. Dietrich, J. Janek, W. Schnick, *Chem. Eur. J.* **2017**, *23*, 2185.
- [40] R. D. Shannon, *Acta Crystallogr. Sect. A* **1976**, *32*, 751.
- [41] J. Cumby, J. P. Attfield, *Nat. Commun.* **2017**, *8*, 14235.
- [42] M.-H. Fang, C. O. M. Mariano, P.-Y. Chen, S.-F. Hu, R.-S. Liu, *Chem. Mater.* **2020**, *32*, 1748.
- [43] G. Kresse, J. Furthmüller, *Comput. Mat. Sci.* **1996**, *6*, 15.
- [44] G. Kresse, J. Furthmüller, *Phys. Rev. B* **1996**, *54*, 11169.
- [45] G. Kresse, J. Hafner, *Phys. Rev. B* **1993**, *47*, 558–561.
- [46] K. Osamura, K. Nakajima, Y. Murakami, P. H. Shingu, A. Ohtsuki, *Solid State Commun.* **1972**, *11*, 617.
- [47] S. T. Tan, B. J. Chen, X. W. Sun, W. J. Fan, H. S. Kwok, X. H. Zhang, S. J. Chua, *J. Appl. Phys.* **2005**, *98*, 013505.
- [48] R. Suhrmann, K. Clusius, *Z. Anorg. Allg. Chem.* **1926**, *152*, 52.
- [49] A. Stock, H. Grüneberg, *Ber. Dtsch. Chem. Ges.* **1907**, *40*, 2573.
- [50] H. Huppertz, *Z. Kristallogr. Cryst. Mater.* **2004**, *219*, 330.
- [51] Bruker-AXS, APEX3, Vers. 2016.5-0, Karlsruhe (Germany), **2016**.
- [52] Bruker-AXS, XPREP Reciprocal Space Exploration, Vers. 6.12, Karlsruhe (Germany), **2001**.
- [53] SAINT, Data Integration Software, Madison, Wisconsin (USA) **1997**.
- [54] G. M. Sheldrick, *Acta Crystallogr. Sect. C* **2015**, *71*, 3.
- [55] G. M. Sheldrick, *SHELXS-97 Program of the Solution of Crystal Structure*, University of Göttingen, Göttingen **1997**.
- [56] K. Momma, F. Izumi, *J. Appl. Crystallogr.* **2011**, *44*, 1272.
- [57] A. A. Coelho, TOPAS-Academic v4.1, Brisbane **2007**.
- [58] P. E. Blochl, *Phys. Rev. B* **1994**, *50*, 17953.
- [59] G. Kresse, D. Joubert, *Phys. Rev. B* **1999**, *59*, 1758.
- [60] J. P. Perdew, K. Burke, M. Ernzerhof, *Phys. Rev. Lett.* **1996**, *77*, 3865.
- [61] P. Pulay, *Chem. Phys. Lett.* **1980**, *73*, 393.

Manuscript received: July 2, 2024

Accepted manuscript online: July 22, 2024

Version of record online: September 9, 2024